This research is focused on increasing the reliability of Fe-11Al-Mn by combining the properties of Mn and the superiority of Fe-Al-C under cryogenic temperature. Three Fe-11Al-Mn alloys with compositions of 15 wt % Mn (F15), 20 wt % Mn (F20), and 25 wt % Mn (F25) were investigated. The cryogenic process uses liquid nitrogen in a temperature range of 0–196 °C. Hardness testing using the Vickers method and SEM was used to analyze the microstructure. X-ray diffraction (XRD) testing was conducted to ensure the Fe-11Al-Mn alloy phase and corrosion testing was carried out using the three-electrode cell polarization method. With the addition of Mn, the Vickers hardness of the Fe-11Al-Mn alloy decreased from 331.50 VHN at 15 wt % to 297.91 VHN at 25 wt %. The value of tensile strength and fracture elongation values were 742.21 MPa, 35.3 % EI; 789.03 MPa, 41.2 % EI; and 894.42 MPa, 50.2 % EI, for F15, F20, and F25, respectively. An important factor for improving the performance of cryogenic materials is the impact mechanism. The resulting impact toughness increased by 2.85 J/mm^2 to 3.30 J/mm^2 for F15 and F25, respectively. The addition of the element Mn increases the corrosion resistance of the Fe-11Al-Mn alloy. The lowest corrosion rate occurs at 25 % wt Mn to 0.016 mm/year. Based on the results, the F25 alloy has the highest mechanical and corrosion resistance of the three types of alloys equivalent to SS 304 stainless steel. The microstructure of Fe-11Al-Mn alloy was similar between before and after cryogenic temperature treatment, this condition showed that the microstructure did not change during the process. From the overall results, the Fa-11Al-Mn alloy is a promising candidate for material applications working at cryogenic temperatures by optimizing the Mn content

Keywords: Fe-11Al-Mn, Microstructure, Mechanical characteristics, Impact, Corrosion resistance, Cryogenic temperature

UDC 620
DOI: 10.15587/1729-4061.2021.243236

DEVELOPMENT OF FE-11AL-XMN ALLOY STEEL ON CRYOGENIC TEMPERATURES

Ratna Kartikasari
Doctor of Mechanical Engineering, Associate Professor*
Adi Subardi
Corresponding author
Doctor of Materials Science and Engineering, Assistance Professor*
E-mail: subardi@itny.ac.id
Andy Erwin Wijaya
Doctor of Mines Engineering, Assistance Professor
Department of Mines Engineering**
*Department of Mechanical Engineering**
**Institut Teknologi Nasional Yogyakarta
Jl. Babarsari, Caturtunggal, Depok, Sleman, Daerah Istimewa Yogyakarta, Indonesia, 55281

Received date 02.09.2021
Accepted date 12.10.2021
Published date 29.10.2021

How to Cite: *Kartikasari, R., Subardi, A., Wijaya, A. E. (2021). Development of Fe-11Al-xMN alloy steel on cryogenic temperatures. Eastern-European Journal of Enterprise Technologies, 5 (12 (113)), 60–68. doi: https://doi.org/10.15587/1729-4061.2021.243236*

1. Introduction

The development of food technology demands that commodities remain fresh and healthy both during storage and processing. Cryogenic technology provides the best solution where food is frozen at freezing point therefore it lasts longer. It has been found that cryogenic freezing technology provides several advantages compared to conventional freezing, cryogenic technology can prevent the destruction of adenosine triphosphate (ATP) in fresh seafood products during the storage period, can accelerate the freezing of food products such as meat and eggs, inhibits the growth of microorganisms that destroy food products, prevent damage to the nutrition of food products. Cryogenic-based technology is also widely applied in various fields such as metallurgy, chemistry, petrochemical, power generation industry, and rocket propulsion, and food processing [1].

In the medical field, cryogenic technology plays a vital role in surgical operations by utilizing cryogenic temperatures to separate bad cells or cancer cells, while in the field of genetic engineering, cryogenic technology provides an opportunity for cells to survive. The use of low-temperature gases in a liquid state such as nitrogen, oxygen, and carbon dioxide is a necessity in cryogenic technology [2].

Handling of these materials is quite complicated and potential problems are avoided. Because liquefied gas is considered dangerous, during transportation and uses it requires safety guarantees. Until this period, research on the application of cryogenic technology is focused on the design of containers or cooling jackets, also on temperature stability along with the design of the controller, and the most recent one is an effort to find the best material to be used as a cryogenic cooling container or jacket including the cryogenic vacuum pipe.

Work [3] investigated the 300 series austenitic stainless steel that is widely used for cryogenic applications due to its high strength and toughness at low temperatures. These alloys generally contain chromium (Cr) ranging from 18–21 % and nickel (Ni) 9–14 %. However, not the majority of austenitic stainless steels can be used below cryogenic temperatures because some austenitic stainless steels change the structure from FCC to BCC resulting in decreased ductility and toughness. Another issue with austenitic stainless steel is the high cost of elemental Ni and the limitation of Cr sources around the world.

Materials experts have made numerous attempts to identify replacement alloys for expensive Cr alloys and Ni-based alloys. The benefits of high austenitic Mn steels, including low cost, high strength, high ductility, and toughness, have been developed for cryogenic applications in the liquefied natural gas industry. The research of [4] demonstrated the Fe-5Al-xMn-based alloy steel has physical and mechanical

properties according to material requirements working at cryogenic temperatures. Alloy Fe-5Al-xMn (25 wt. % Mn) has high impact toughness, high hardness, and high corrosion resistance recorded at 0.036 mm/year.

Thus, it is relevant to develop materials operating at cryogenic temperatures based on Fe-11Al-xMna alloys. To reduce various obstacles, including dependence on Cr-based alloy steels which are in limited supply.

2. Literature review and problem statement

Described in work of [3], the materials that are usually ductile at atmospheric temperatures but tend to be very brittle at cryogenic temperatures, whereas other materials can increase ductility. Other factors need to be considered, especially the joining technique used must be chosen properly therefore that it does not change the basic properties of the material. The properties of different materials at low temperatures depend on various factors such as crystal structure, grain size, tendency to absorb contaminants from the atmosphere, heat treatment, melting process, welding, and deformation. FCC metals are widely used because of their moderately low-temperature toughness, whereas BCC metals exhibit a ductile-brittle transition. Austenitic stainless steel (9 % Ni) are commonly used in large-scale industries, although significant effort has been directed towards replacing expensive Ni-based alloys with low-cost high Mn steels of comparable strength, ductility, and toughness.

The authors of [5] declared that the Fe-Al-Mn alloy system is a low-cost austenitic type stainless steel due to the abundance of Al in the world. Aluminum (Al) functions as a structural stabilizer of ferrite [6], the addition of this element in the alloy system can increase oxidation and reduction resistance. The addition of Mn to the alloy system stabilizes the austenite structure, improves heat workability and ductility [7].

The addition of 2 % Mn and Mo elements can increase ductility and toughness when the addition of 0.5 % Si elements is proven to increase the tensile strength of Fe-7.5Al-5Mn [8]. The high Mn content (>35 %) causes the alloy to tend to be brittle due to the formation of the β-Mn phase. When Al content is above 12 %, the alloy tends to form a ferritic stainless steel alloy system. The addition of Si to the Fe-Al-Mn alloy system causes a decrease in ductility due to the formation of carbide [9]. The decrease in ductility can be reduced by decreasing the Al content up to 5 %. The mechanical properties of Fe-Al-Mn alloys are influenced by the perfection of the austenite alloy structure which is determined by the content of Mn (>15 %) and Al (3–6 %). In addition, during the solution heat treatment process until quenching, the κ-carbide precipitate will be formed if the content of C and Al elements is sufficient [10].

The authors of [11], when compared to conventional steels, mechanical properties at cryogenic temperatures show excellent results, which can be related to the activation of certain deformation mechanisms. Similar results in work [12, 13], the Fe-Al-Mn alloys exhibit outstanding mechanical properties at low temperatures, therefore Fe-Al-Mn alloys can be considered potential new cryogenic alloys. Due to its improved room temperature yield strength (380 MPa) and impact toughness value (130 J/cm^2) at 77 K, the Mn-Al-Si-C austenitic steels offer promising mechanical characteristics that can substitute austenitic Fe-Ni steels.

Paper [14] investigated the effect of Mn (19 and 22 wt. %) and Al (0 and 2 wt. %) contents on the tensile and impact properties of Charpy at room temperature and cryogenics. Martensite is not found in steel with added Al, the formation of many twin deformations results in high Charpy impact energy. The effect of deep cryogenic treatment (DCT) and critical annealing (IA) on the microstructural evolution and mechanical properties of hot-rolled manganese transformation-induced plasticity (TRIP) steels has been systematically investigated. Mechanical properties increased significantly with increasing mechanical stability of austenite, yield strength of 807 MPa, the tensile strength of 1650 MPa, and total elongation of 25.3 %, which is described in [15]. Study [16] investigated the effect of cryogenic treatment on the mechanical properties and microstructure of AISI 4340 steel. Neutron diffraction showed that the transformation of austenite was restrained to martensite, possibly forming carbides during tempering. These conditions are a major factor in increasing the hardness and fatigue resistance of the cryogenically treated specimens.

The authors [17] proposed the Charpy impact toughness of three austenitic high Mn steel tested at room temperature and cryogenically. The majority of martensite is formed in 0.4C–22Mn steel via the transformation-induced plasticity (TRIP) mechanism. The twinning-induced plasticity (TWIP) mechanism increases Charpy's toughness compared to 0.4C–24Mn and 0.4C–26Mn steel. Another author [18] reported the maximal strength of a specimen extruded to a strain of 1.36 and tested in liquid helium was 2.6 GPa. The findings indicate that hydrostatically extruded austenitic stainless steels are potential materials for cryogenic components that are relatively small and heavy-duty.

Study [19] illustrates the tensile test of twinning-induced plasticity steels of various grain sizes at cryogenic temperatures. At 123 K, grain refinement improved tensile elongation, yield strength, and ultimate tensile strength significantly. Work [20] reported the yield strength of the steel with the double reinforcing structure is raised by 86 MPa compared to the soft structure, the cryogenic impact energy (–196 °C) is reduced by only 17 J. Improved tensile properties of resistant steel duplex ferrite and austenite rust at cryogenic temperatures is affected by martensite transformation induced deformation, simultaneous deformation of ferrite and austenite, ductile fracture as illustrated in [21].

Austenitic high Mn steels containing about 20 wt. % Mn have been developed, but few studies have been carried out on the optimization of Mn elements through combined testing of impact toughness and corrosion resistance. This work will formulate the ratio of Mn content that has a significant effect on the performance of Fe-11Al-xMn alloys (x=15 wt. %, 20 wt. %, and 25 wt. %) and analyze the impact ability of the material at cryogenic temperatures. In this work, the austenitic microstructure was prepared by varying the Mn content and the Charpy impact was examined at room temperature and cryogenically.

3. The aim and objectives of the study

The aim of the study is to development of Fe-11Al-xMn [x=15 wt %, 20 wt %, and 25 wt. %] alloys for a cryogenic cooling container or jacket including the cryogenic vacuum pipe.

To achieve this aim, the following objectives are accomplished:

– modify the structure of Fe-11Al-Mn by adding Mn content (15 wt %, 20 wt %, and 25 wt %);

– investigate the mechanical properties (hardness, tensile strength, and impact);

– investigate the physical properties of corrosion resistance;

– investigate the microstructure & the impact performance at the cryogenic temperature.

4. Materials and methods

The raw materials for smelting are Fe-C, Fe-Mn-C medium, pure Al, and mild steel scrap. The composition calculation is conducted manually with material balance and smelting using a vacuum furnace. The wooden pattern is in the form of an ingot measuring 20×3×3 cm and is in the shape of a ball with a diameter of 30 mm, followed by making resin molds.

The smelting of the Fe-Al-Mn alloy begins with the manufacture of a starter block, namely the smelting of mild steel, Fe-Mn-C medium, and Fe-C with a target composition of 0.5 % C and with variations of Mn 15, 20, and 25 wt. %. The next stage is the smelting of the cylinder block with Al in an induction furnace with argon gas shielding. Composition control is carried out with a chill tester before pouring. Then, the molten metal is poured into the ingot mold manually using a ladle. Inspection of castings is carried out to ensure that the Fe-Al-Mn alloy castings are free from defects.

Specimen preparation for the characterization of Fe-11Al-xMn alloys included microstructure testing, tensile testing, hardness testing, impact testing, and corrosion resistance testing with three-electrode cell polarization. Microstructure testing was carried out with an optical microscope and SEM coupled with EDS-EDAX. The XRD test was carried out to confirm the Fe-Al-Mn alloy phase. Corrosion testing was carried out using the 3-electrode cell polarization method in a 0.5 % HCl solution.

5. Result of Experiment

5. 1. Modify the structure of Fe-5Al-1C

5. 1. 1. The chemical compositions

The XRD patterns for F15, F20, and F25 are shown in Fig. 1. The specimen synthesis process was successful, there were no peaks caused by impurities. The XRD pattern in Fig. 1, *a–c* shows that the Fe-11Al-15 Mn alloy consists of two dominant phases, austenite (γ) at an angle 2-theta of 45° and ferrite (FeAl) at an angle 2-theta of 75°. At 20 % Mn the austenite phase increased while the ferrite (FeAl) phase decreased significantly.

At 25 % Mn almost all austenite phases, the ferrite phase is nearly invisible. The EDS curve reveals that Fe has a high intensity, implying that the γ Fe phase is equally distributed. The γ Fe phase has an FCC crystal structure and has a crystal plane (111), while at an angle 2-theta of 75° it has a crystal plane (220). Chemical composition test to obtain the percentage of chemical elements contained in the specimen. The elements in the Fe-Al-Mn alloy greatly affect their mechanical properties. The Mn element in the specimen is expected to replace the properties of the Cr element in the cryogenic materials. Visually, the higher the Mn content in the Fe-Al-Mn alloy shows grayish-white castings (Fig. 2).

Table 1 presents the chemical composition of the three specimens is 15.354 % (F15), 21.280 % (F20), and 25.320 % (F25) which showed that they were consistent with the ratio of Mn content applied to these specimens.

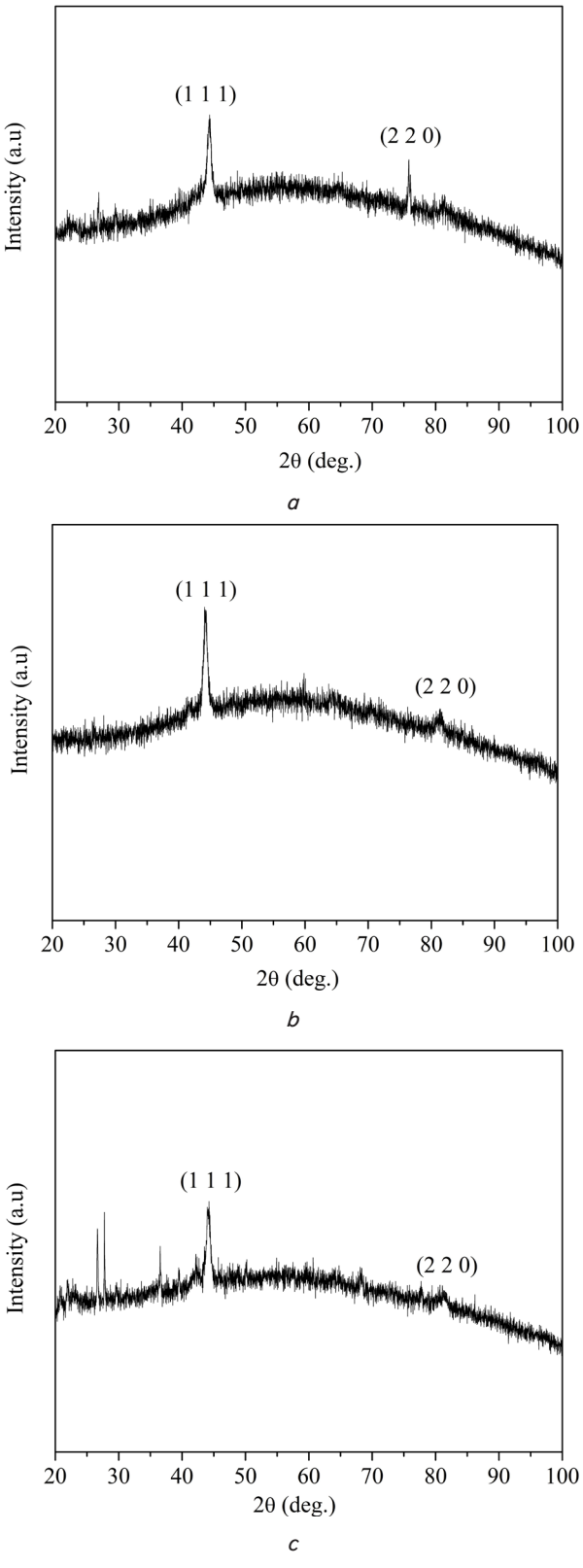

Fig. 1. Room-temperature XRD pattern: *a* – F15; *b* – F20; *c* – F25

Fig. 2. Castings of Fe-Al-Mn alloys

The overall composition test results met the expected target and the smelting method has reached the alloy composition. The Fe element dominates the Fe-11Al-Mn alloy with a content of 81.978 % (F15), 74.299 % (F20), and 71.403 % (F25) respectively. Other elements in low percentage are C, Si, P, S, Ni, Cr, and Mo. From this group, only Si was detected in higher percentages of 1.839 % (F15), 2.632 %, and 1.165 % (F25).

Table 1

Chemical alloy composition

Element	F15	F20	F25
Fe	81.978	74.299	71.403
Al	9.096	10.473	11.165
Mn	15.354	21.280	25.320
C	0.086	0.932	0.846
Si	1.839	2.632	1.165
P	0.043	0.051	0.056
S	0.018	0.013	0.006
Ni	0.057	0.051	0.034
Cr	0.150	0.151	0.717
Mo	0.034	0.037	0.126

5. 1. 2. The microstructure of Fe-11Al-Mn alloys

Microstructure testing was carried out with an optical microscope with a magnification of 500×. Etching was conducted using HCl, HNO_3, and HF etching fluids. The microstructure is shown in Fig. 3, *a–c*. The alloy phase will reach 100 % ferritic at Al content above 10 %. The microstructure of the three specimens (Fig. 3, *a–c*) was detected as ferrite, austenite, and iron carbide (cementite). In Fig. 3, *a*, the color of the ferrite structure is opaque with fine grains and the white phase is a cementite structure arranged in coarse grains with sizes ranging from 5–10 μm in a continuous formation. Meanwhile, the green one is the austenite phase that occupies the ferrite and carbide phases.

As shown in Fig. 3, *c*, the steel alloy with Mn content of 25 wt % produces a carbide structure in a dominating area compared to the ferrite and austenite phases. The carbide phase is in the range of 20–25 m which occupy between the ferrite and austenite phase.

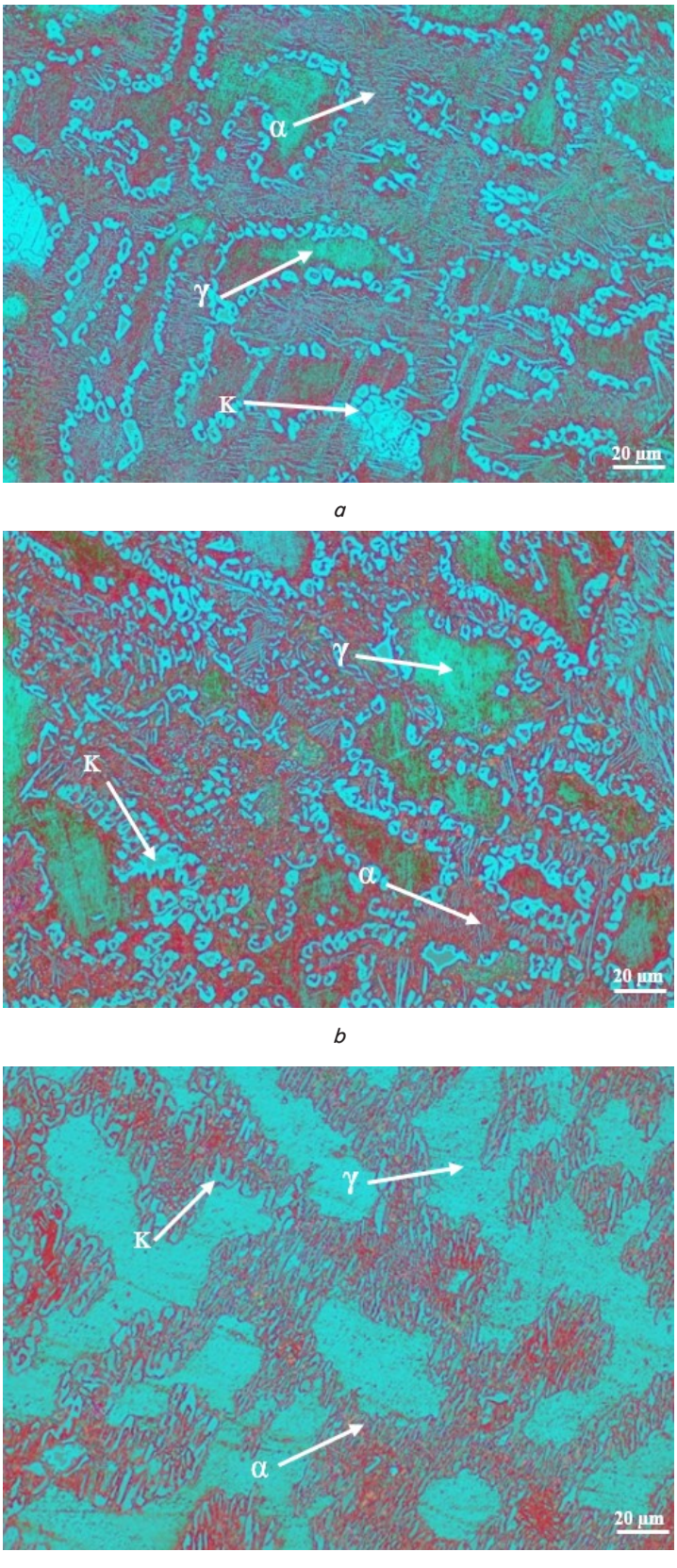

Fig. 3. Microstructure: *a* — F15; *b* — F20; *c* — F25

5. 2. Mechanical properties

5. 2. 1. Hardness and tensile strength

Fig. 4 shows that increasing the content of Mn from 15 % to 25 % in Fe-Al-Mn alloys causes a relatively small decrease

in hardness ranging from 0.5–5 %. The highest hardness value occurred at 15 % Mn content of 225.5 VHN and the hardness value continued to decrease with increasing Mn content until the lowest hardness occurred at 25 % Mn content reaching 297.907 VHN or a decrease in hardness of 5 %.

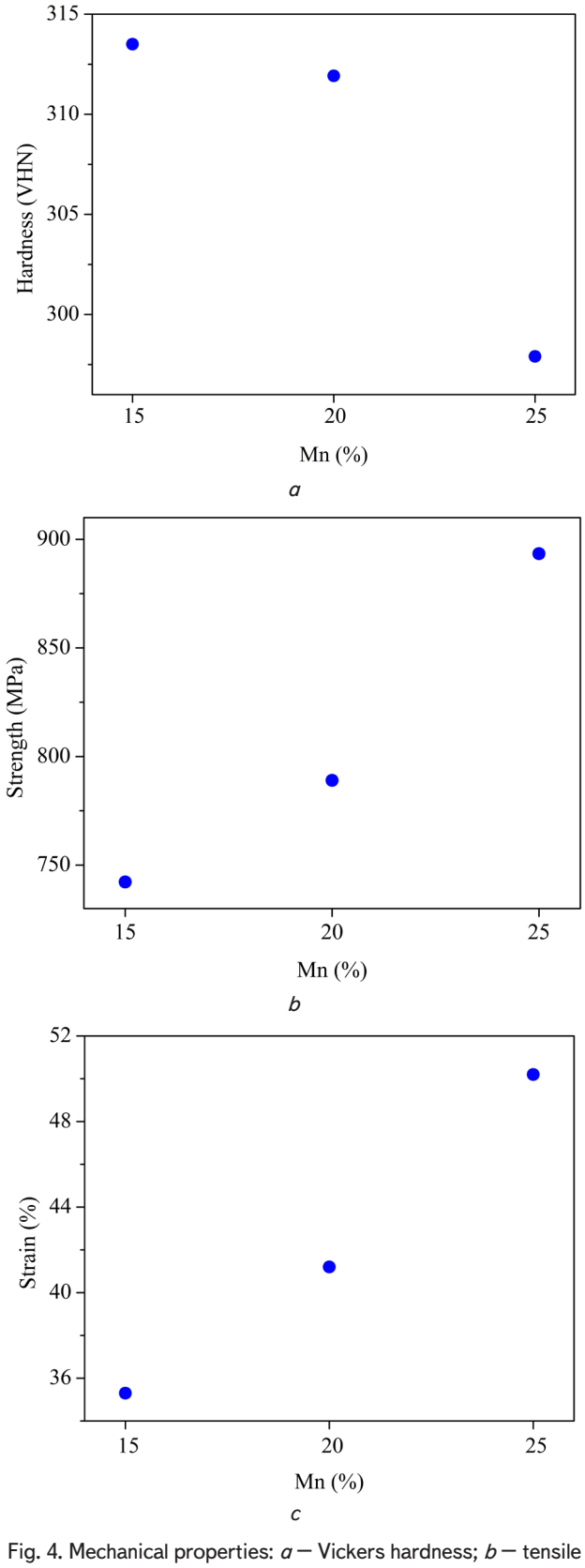

Fig. 4. Mechanical properties: *a* — Vickers hardness; *b* — tensile strength; *c* — fracture elongation values of F15, F20, and F25

Overall, the tensile strength of Fe-Al-Mn alloys is in the range of 731.3–885.07 MPa, the higher the Mn content, the higher the tensile strength and strain (Fig. 4, *b*, *c*). Tensile strength in specimens with 15 % Mn content (F15) reached 742 MPa. The next composition, which is 20 wt. % Mn and 25 wt. % Mn, has a higher strain than SS 304, which is 41.2 % and 50.2 %. The higher strain at higher Mn content was due to lower lattice density at higher Mn content. The Mn atom occupies the position of the Fe atom which is larger than the Fe atom.

The increase in strength followed by an increase in strain is one of the advantages of Fe-Al-Mn alloys compared to conventional stainless steels. This phenomenon is due to the combined effect of the presence of the elements Al, Mn, and C in the alloy system. The formation of a solid solution of Fe-Al-Mn causes a significant increase in strength and strain at the same period.

5. 2. 2. Impact properties

Fig. 5 shows the effect of Mn content on the impact toughness for the Fe-11Al-Mn alloys. The addition of Mn to Fe-Al-Mn alloys increased the toughness significantly up to 3.10 J/mm^2 at 20 % Mn and reached the highest toughness at 25 % Mn content of 3.3 J/mm^2. The addition of Mn to the Fe-Al-C alloy system increased the strength and toughness significantly. The increase in strength followed by a significant increase in ductility resulted in a very high increase in toughness. This condition is caused by changes in the microstructure of the alloy towards austenitic. The alloy composition with 25 % Mn produces a toughness value that is almost equivalent to that of conventional SS 304 as cast stainless steel of 3.12 J/mm^2.

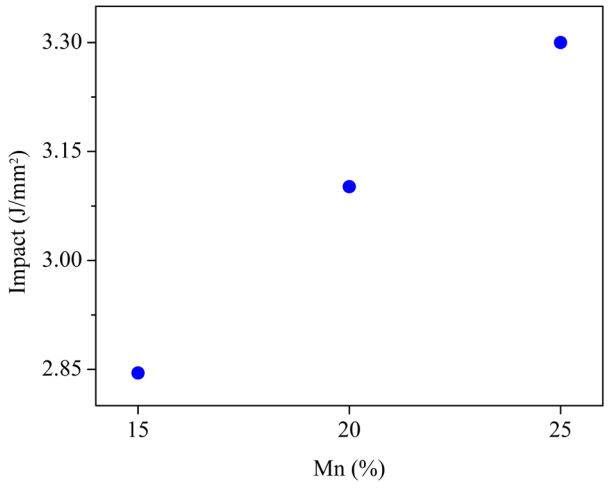

Fig. 5. Effect of Mn content on the impact toughness for the Fe-11Al-Mn alloys

Fig. 6 shows the impact (toughness) effect on the Mn content for the Fe-11Al-xMn alloys. The surface of the F25 specimen has a ductile fracture which is not present in the F15 and F20 specimens.

The toughness value of Fe-Al-Mn alloy is 0.18 J/mm^2 (5.8 %) higher than that of SS 304. The substitution of Mn in the Fe system is the cause of the significant increase in toughness significant. The difference in the distance between atoms (lattice) causes the movement of atoms in the material when receiving a load to become more flexible. Mechanically, the toughness, ductility, and strain are higher.

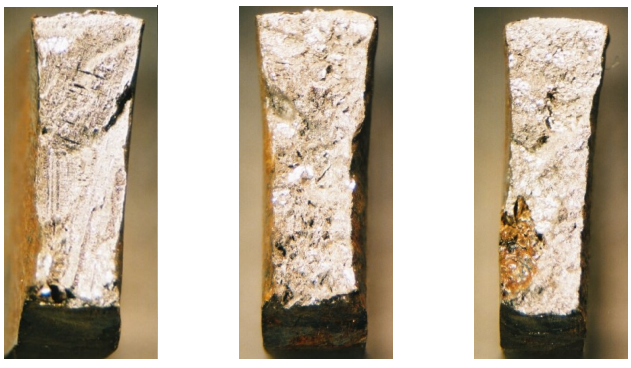

a *b* *c*

Fig. 6. Fracture surface after the impact test:
a — F15; *b* — F20; *c* — F25

5. 3. Physical properties of Corrosion Resistance

Corrosion testing was conducted by calculating the corrosion rate of the samples using the weight difference before and after soaking in a 0.5 % HCl (chloride acid) solution. Fig. 7 shows the corrosion rate of Fe-Al-Mn-C alloy in the range of 0.016–0.031 mm/yr in 0.5 % NaCl media, with a tendency for the corrosion rate to decrease with increasing Mn content in the alloy.

Table 2 shows the corrosion rates for the F15, F20, F25, and SS 304 specimens. The Mn element in the Fe-11Al-1C alloy has a significant impact on corrosion resistance. The alloy with the lowest element of Mn (15 %) produces the highest corrosion resistance compared to other specimens.

The corrosion resistance of this alloy up to 20 % Mn is included in the very good category, while the alloy with 25 % Mn content is included in the extraordinary category. The lowest corrosion rate of Fe-Al-Mn-C alloy occurs at 25 % Mn content, which is 0.016 mm/yr, lower than the corrosion rate of SS 304 stainless steel, which is 0.025 mm/yr. The decrease in the corrosion rate was quite significant, reaching 78.67 %.

Table 2

Corrosion rate values for F15, F20, F25, and SS 304

Specimens	I Corr (μA/cm^2)	Corrosion Rate (mm/y)
F15	3.66	0.031
F20	2.85	0.024
F25	1.95	0.016
SS 304	3.05	0.025

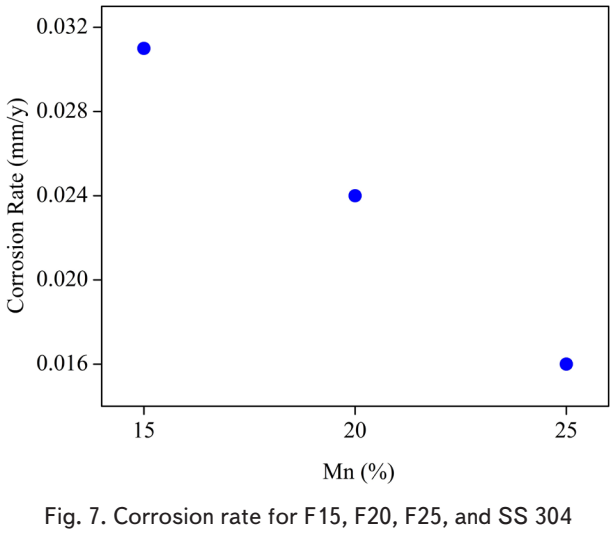

Fig. 7. Corrosion rate for F15, F20, F25, and SS 304

5. 4. Microstructure And Impact Properties of Fe-11Al-xMn at Cryogenic Temperatures

5. 4. 1. Microstructure of Fe-11Al-xMn at Cryogenic Temperatures

The cryogenic process was carried out using liquid nitrogen at various temperatures of 0 °C, –100 °C, and –196 °C for 2 hours. This process is carried out to determine the resistance of the material to cryogenic temperatures. The test specimens were immersed in liquid nitrogen at various temperatures and times. To determine the phenomenon at room temperature and slightly above room temperature, the specimens were tested at temperatures of 100 °C and 200 °C. Fig. 8 shows the microstructure of Fe-Al-Ma alloy after the cryogenic process, similar to the microstructure before the cryogenic process (Fig. 3).

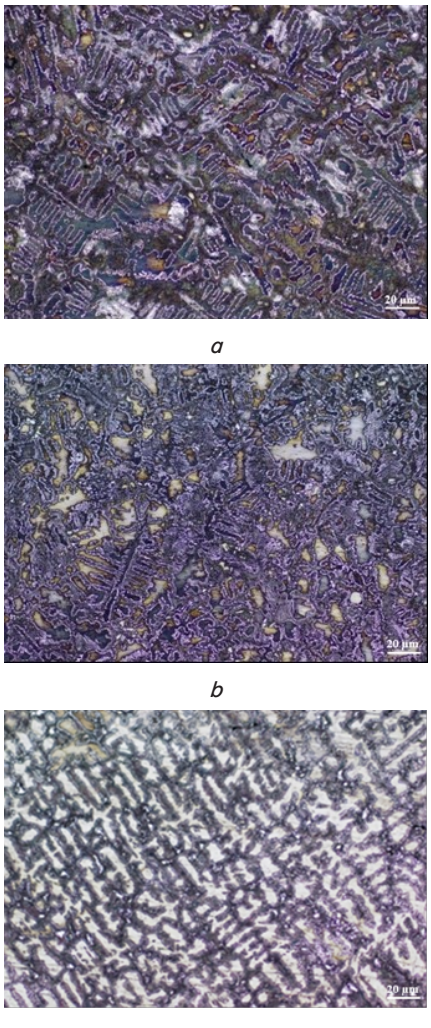

a *b* *c*

Fig. 8. Microstructure of Fe-11Al-Mn alloy after cryogenic treatment for: *a* — F15; *b* — F20; *c* — F25

The microstructure of the three specimens F15, F20, and F25 was unaffected by the cryogenic treatment. This shows that the cryogenic treatment has a negligible effect on the microstructure. The high C concentration in this alloy prevents austenite from converting to martensite.

5. 4. 2. The Impact Properties of Fe-11Al-Mn at Cryogenic Temperatures

The purpose of the Charpy impact test is to determine the brittleness or ductility of a material (specimen) to be tested

by loading suddenly on the object to be tested statically. The Charpy impact test also known as the Charpy v-notch test is a standard high strain rate test that determines the amount of energy absorbed by a material during fracture. Fig. 9 shows the impact properties of the F15, F20, F25, and SS 304 specimens at various temperatures up to –190 °C. At 190 °C, the impact values are 2.79 J/mm^2 (F15), 3.19 J/mm^2 (F20), 3.35 J/mm^2 (F25), and 3.13 J/mm^2 (SS 304). The impact value didn't considerably decline at -190 °C, notably for the F20, F25, and SS 304 specimens, which are 3.09 J/mm^2, 3.15 J/mm^2, and 3.11 J/mm^2, respectively.

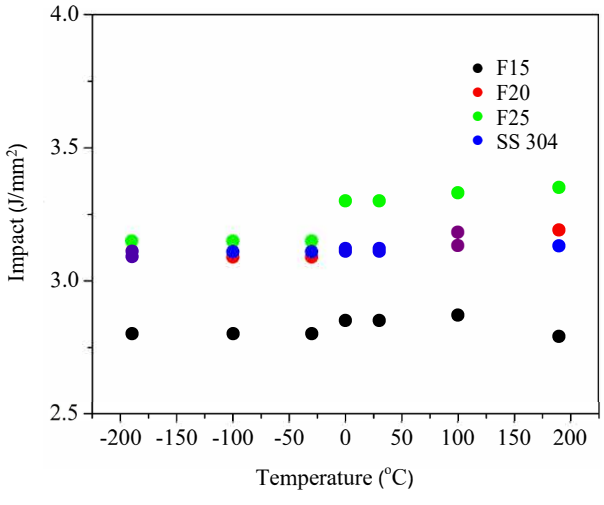

Fig. 9. The effect of temperature on impact for Fe-Al-Mn alloy

The impact values of Fe-Al-Mn and SS 304 specimens in the temperature range of 190 °C and –190 °C are listed in Table 3. The impact values of the four specimens at temperatures below 0 °C to –190 °C did not change and were stable.

Table 3

Impact values for Fe-Al-Mn alloys and SS 304 stainless steel

Temp. (°C)	Impact (J/mm^2)			
	F15	F20	F25	SS 304
190	2.79	3.19	3.35	3.13
100	2.87	3.18	3.33	3.13
30	2.85	3.11	3.30	3.12
0	2.85	3.11	3.30	3.11
–30	2.80	3.09	3.15	3.11
–100	2.80	3.09	3.15	3.11
–190	2.80	3.09	3.15	3.11

Absorbed energy is a measure of the toughness of a given material and depends on the brittle-ductile transition temperature. This method is widely used in safety-critical industries because it is easy to prepare and perform. Fig. 9 shows the real fracture surface changes of the 15 %, 20 %, and 25 % Mn compositions. The higher the Mn content indicates the higher ductility, the necking is very clearly presented at the Mn content of 20 % and 25 %. At cryogenic temperatures, Fe-Al-Mn alloy did not cause significant changes in microstructure and mechanical properties. From the overall results, it can be concluded that this alloy is resistant to cryogenic temperatures and can be used for low-temperature applications.

6. Discussion of experimental results

The chemical composition data of alloy specimens F15, F20, and F25 are high alloy steel FA-Al-Mn-Si as shown in Table 1. This alloy steel contains elements of carbon, aluminum, manganese, silicon, phosphorus, and sulfur. The element Mn plays a role in preventing precipitation in aluminum alloys which increases corrosion resistance. The microstructure, grain size, and mechanical strength of metal alloys are influenced by the composition of the alloy applied. Impurities in the alloy system are elements that can be ignored because they do not affect the behavior of the alloy metal.

Fig. 3, *a* shows the microstructure of Fe-11Al-15Mn alloy consisting of austenite, ferrite (FeAl) [22] structure, and intermetallic compound (Fe,Mn)3AlC (κ phase) surrounding austenite grains. In Fig. 3, *b*, where the 20 % Mn content presents that the ferrite structure is decreasing followed the area of the increasing phase. Fig. 3, *c* shows that there is a change in the pattern or shape of the austenite and ferrite grains. The austenite structure dominates, the ferrite structure disappears and shows the dendritic structure in a wider area. The appearance of double phases in the three compositions was due to the relatively high Al content and insufficient Mn content to reach the perfect austenite phase [23]. Low and medium Mn content also cannot change the ferritic structure into perfect austenite [24]. The addition of 5–10 % Mn to the Fe-Al-C alloy system forms α/γ duplex structure [7]. The ability of Mn to form and stabilize the austenite structure is only half that of the element Ni, these conditions require Mn in sufficient quantities to obtain a perfect austenite structure [25]. Mn is dissolved in the Fe system as a solid solution with a disordered FCC structure [26]. The presence of Al atoms in the system changes the disordered FCC structure to ordered FCC and C atoms cause the formation of the K (Fe,Mn)3AlC phase. This κ phase surrounds the austenite phase in the α/γ duplex system [27].

Based on structural changes that occur in the range of increasing Mn content, the increase in the area of the austenite structure formed causes a decrease in hardness, this condition is equivalent to a decrease in tensile strength that occurs due to an increase in Mn content in the alloy [28]. The Mn atoms occupying the position of the Fe atom shift the Al atoms in the Fe-Al-Mn-C alloy system causing the lattice density to decrease so that the hardness level decreases [26]. Due to the size of the Mn atom (1.79 Angstrom) is smaller than the size of Al (1.82 Angstrom) and closer to the size of the Fe atom (1.72 Angstrom), the decrease in hardness is not significant. Compared with austenitic stainless steel SS 304 with a hardness value of 203 VHN, the composition with the closest hardness value is 25 % Mn alloy. It was observed from the microstructure that the alloy formed with 25 % Mn was a perfect austenite structure.

Mechanical properties and fracture elongation values for F15, F20, and F25 are shown in Fig. 4. Compared to austenitic stainless steel SS 304 with a tensile strength of 552.5 MPa, Fe-Al-Mn alloy achieved a higher tensile strength than SS 304. Mn elements in steel play a role in increasing strength, the results of this study also concluded that the higher the Mn content in Fe-11Al-Mn alloys have higher tensile strength [28]. Besides that, the austenitic structure which is stable at room temperature and increasing with higher Mn content causes higher strength than SS 304, conventional austenitic stainless steel [5].

The strengthening mechanism using Mn and Al elements in the Fe-Al-Mn alloy system can be explained as follows, Mn in the Fe crystal system occupies an equivalent position with Fe. This crystal system is FCC (γ). The element Al occupies the corner points of the cubic crystal while Fe and Mn atoms occupy the center point of the side of the cubic crystal system (γ') [7]. The change in crystal structure from disordered to γ' ordered (Fig. 3) causes a significant increase in tensile strength. At levels of Mn below 15 %, some of the γ' ordered will be transformed into the (Fe, Mn)3AlC phase. Meanwhile, at 25 % Mn content, the microstructure changed to austenite (γ) completely [29]. The formation of a single-phase from several of these elements causes a stress field interaction between soluble atoms and dislocations, this condition requires greater mechanical energy to form plastic deformation [26].

Fig. 7 shows the corrosion rates for F15, F20, F25, and SS 304 stainless steel. As the Ni element in conventional stainless steel, the Mn element in the Fe-Al-Mn-C alloy besides playing a role in increasing strength and toughness, the Mn element also plays a role in stabilizing the austenite structure at room temperature and also plays a role in increasing the corrosion resistance of the alloy.

Fig. 8 presents the microstructure of Fe-11Al-Mn alloy after cryogenic treatment. The microstructure of the Fe-Al-Mn alloy system is relatively stable in the temperature range of 0 °C to 200 °C [3]. Strong bonds between atoms lead to high phase stability. The microstructure of the Fe-Al-Mn alloy after the cryogenic process using SEM showed that the structure of austenite, ferrite, and kappa had almost the same pattern and size as the original alloy. It can be concluded that the Fe-Al-Mn alloy does not undergo a brittle-ductile transition in the temperature range of –200 °C to 200 °C. This condition is similar to the phenomenon in SS 304 stainless steel.

Fig. 9 shows the effect of temperature on impact for Fe-Al-Mn alloy The transition curve of Fe-Al-Mn alloy is horizontal, very similar to the transition curve of SS 304 stainless steel and the impact value is close to the impact value of SS 304. The highest toughness value of Fe-11Al-25Mn alloy is 3.3 J/mm^2, the value is still above the toughness value of SS 304 stainless steel, which is 3.12 J/mm^2.

Overall, this research is still limited to testing the microstructure and impact toughness under cryogenic treatment and testing of mechanical properties has not been carried out on Fe-11Al-Mn alloys under cryogenic conditions. In addition, the performance improvement of Fe-11Al-Mn alloy steel requires further development. Heat treatment including surface hardening and age hardening is a commonly applied method that can improve ductility, wear resistance, and hardness.

7. Conclusions

1. It has been determined that the alloy structure of Fe-11Al-Mn to Fe-11Al-xMn (F15, F20, F25) has been successfully developed with the addition of Mn content.

2. It has been determined that the tensile test shows that the higher the Mn content indicates the higher the tensile strength, the tensile stress of the F25 specimen exceeds SS 304.

3. The corrosion resistance of Fe-Al-Mn alloys increases significantly with increasing Mn content. Specimen F25 showed the lowest corrosion rate of 0.016 mm/year suitable as a material working under cryogenic temperature.

4. The results of the cryogenic temperature microstructure test showed that the microstructure of the Fe-Al-Mn alloy was almost the same between the specimens before and after the cryogenic process. Strong bonds between atoms lead to high phase stability. Impact test results are comparable to tensile test data, impact toughness increases with increasing Mn content. These results are consistent with the tensile test data. Specimens treated with a cryogenic temperature of –190 °C, the impact toughness of F25 is 3.15 J/mm^2 which is higher than that of SS304 stainless steel.

Acknowledgments

The study was funded by The Ministry of Research, Technology and Higher Education of the Indonesia Republic "National Institution Research Grant" under Decree number: 185/SP2H/AMD/LT/DRPM/2020.

References

1. Qiu, Y., Yang, H., Tong, L., Wang, L. (2021). Research Progress of Cryogenic Materials for Storage and Transportation of Liquid Hydrogen. Metals, 11 (7), 1101. doi: https://doi.org/10.3390/met11071101
2. Gao, L., Yang, L., Qian, S., Tang, Z., Qin, F., Wei, Q. et. al. (2016). Cryosurgery would be An Effective Option for Clinically Localized Prostate Cancer: A Meta-analysis and Systematic Review. Scientific Reports, 6 (1). doi: https://doi.org/10.1038/srep27490
3. Tjong, S. C. (1986). Stress corrosion cracking behaviour of the duplex Fe-10Al-29Mn-0.4C alloy in 20% NaCl solution at 100 °C. Journal of Materials Science, 21 (4), 1166–1170. doi: https://doi.org/10.1007/bf00553248
4. Kartikasari, R., Subardi, A., Wijaya, A. E. (2021). Development of Fe-5Al-1C alloys for grinding ball. Eastern-European Journal of Enterprise Technologies, 1 (12 (109)), 29–35. doi: https://doi.org/10.15587/1729-4061.2021.225421
5. Shackelford, J. K. (1992). Introduction to Material Science for Engineers. New York: McMillan Publishing Company.
6. Zimmer, J. M., Bailey, W. D. (2006). Pat. No. US4865662A. Aluminum-manganese-iron stainless steel alloy. No. 164,055; declareted: 03.03.1988; published: 12.09.1989. Available at: https://patentimages.storage.googleapis.com/7b/f1/c8/d968e628ccaeeb/US4865662.pdf
7. Frommeyer, G., Drewes, E. J., Engl, B. (2000). Physical and mechanical properties of iron-aluminium-(Mn, Si) lightweight steels. Revue de Métallurgie, 97 (10), 1245–1253. doi: https://doi.org/10.1051/metal:2000110
8. Baligidad, R. G., Prasad, V. V. S., Rao, A. S. (2007). Effect of Ti, W, Mn, Mo and Si on microstructure and mechanical properties of high carbon Fe–10·5 wt-%Al alloy. Materials Science and Technology, 23 (5), 613–619. doi: https://doi.org/10.1179/174328407x158631
9. Heo, Y.-U., Song, Y.-Y., Park, S.-J., Bhadeshia, H. K. D. H., Suh, D.-W. (2012). Influence of Silicon in Low Density Fe-C-Mn-Al Steel. Metallurgical and Materials Transactions A, 43 (6), 1731–1735. doi: https://doi.org/10.1007/s11661-012-1149-x

10. Kim, H., Suh, D.-W., Kim, N. J. (2013). Fe–Al–Mn–C lightweight structural alloys: a review on the microstructures and mechanical properties. Science and Technology of Advanced Materials, 14 (1), 014205. doi: https://doi.org/10.1088/1468-6996/14/1/014205
11. Charles, J., Berghezan, A. (1981). Nickel-free austenitic steels for cryogenic applications: The Fe-23% Mn-5% Al-0.2% C alloys. Cryogenics, 21 (5), 278–280. doi: https://doi.org/10.1016/0011-2275(81)90003-5
12. Charles, J., Berghezan, A., Lutts, A. (1984). High manganese - aluminum austenitic steels for cryogenic applications, some mechanical and physical properties. Le Journal de Physique Colloques, 45 (C1), C1-619–C1-623. doi: https://doi.org/10.1051/jphyscol:19841126
13. Kim, Y. G., Park, Y. S., Han, J. K. (1985). Low temperature mechanical behavior of microalloyed and controlled-rolled Fe-Mn-Al-C-X alloys. Metallurgical Transactions A, 16 (9), 1689–1693. doi: https://doi.org/10.1007/bf02663026
14. Sohn, S. S., Hong, S., Lee, J., Suh, B.-C., Kim, S.-K., Lee, B.-J. et. al. (2015). Effects of Mn and Al contents on cryogenic-temperature tensile and Charpy impact properties in four austenitic high-Mn steels. Acta Materialia, 100, 39–52. doi: https://doi.org/10.1016/j.actamat.2015.08.027
15. Yan, N., Di, H., Misra, R. D. K., Huang, H., Li, Y. (2019). Enhancing austenite stability in a new medium-Mn steel by combining deep cryogenic treatment and intercritical annealing: An experimental and theoretical study. Materials Science and Engineering: A, 753, 11–21. doi: https://doi.org/10.1016/j.msea.2019.01.026
16. Zhirafar, S., Rezaeian, A., Pugh, M. (2007). Effect of cryogenic treatment on the mechanical properties of 4340 steel. Journal of Materials Processing Technology, 186 (1-3), 298–303. doi: https://doi.org/10.1016/j.jmatprotec.2006.12.046
17. Kim, H., Ha, Y., Kwon, K. H., Kang, M., Kim, N. J., Lee, S. (2015). Interpretation of cryogenic-temperature Charpy impact toughness by microstructural evolution of dynamically compressed specimens in austenitic 0.4C–(22–26)Mn steels. Acta Materialia, 87, 332–343. doi: https://doi.org/10.1016/j.actamat.2014.11.027
18. Czarkowski, P., Krawczyńska, A. T., Brynk, T., Nowacki, M., Lewandowska, M., Kurzydłowski, K. J. (2014). Cryogenic strength and microstructure of a hydrostatically extruded austenitic steel 1.4429 (AISI 316LN). Cryogenics, 64, 1–4. doi: https://doi.org/10.1016/j.cryogenics.2014.07.014
19. Koyama, M., Lee, T., Lee, C. S., Tsuzaki, K. (2013). Grain refinement effect on cryogenic tensile ductility in a Fe–Mn–C twinning-induced plasticity steel. Materials & Design, 49, 234–241. doi: https://doi.org/10.1016/j.matdes.2013.01.061
20. Ren, J., Chen, Q., Chen, J., Liu, Z. (2020). Enhancing strength and cryogenic toughness of high manganese TWIP steel plate by double strengthened structure design. Materials Science and Engineering: A, 786, 139397. doi: https://doi.org/10.1016/j.msea.2020.139397
21. Koga, N., Nameki, T., Umezawa, O., Tschan, V., Weiss, K.-P. (2021). Tensile properties and deformation behavior of ferrite and austenite duplex stainless steel at cryogenic temperatures. Materials Science and Engineering: A, 801, 140442. doi: https://doi.org/10.1016/j.msea.2020.140442
22. Nadig, D. S., Bhat, M. R., Pavan, V. K., Mahishi, C. (2017). Effects of Cryogenic Treatment on the Strength Properties of Heat Resistant Stainless Steel (07X16H6). IOP Conference Series: Materials Science and Engineering, 229, 012014. doi: https://doi.org/10.1088/1757-899x/229/1/012014
23. Kim, J.-S., Jeon, J. B., Jung, J. E., Um, K.-K., Chang, Y. W. (2014). Effect of deformation induced transformation of ε-martensite on ductility enhancement in a Fe-12 Mn steel at cryogenic temperatures. Metals and Materials International, 20 (1), 41–47. doi: https://doi.org/10.1007/s12540-014-1010-4
24. Baligidad, R. G., Prasad, K. S. (2007). Effect of Al and C on structure and mechanical properties of Fe–Al–C alloys. Materials Science and Technology, 23 (1), 38–44. doi: https://doi.org/10.1179/174328407x158389
25. Honeycombe, R., W. K., Bhadeshia, H. K. D. (1995). Steels: microstructure and properties. London: Edward Arnold. Available at: https://www.worldcat.org/title/steels-microstructure-and-properties/oclc/33045504
26. Zuazo, I., Brechet, Y. (2009). Microstructure Evolution in Fe-Al-Mn-C lightweight alloys. Laboratory of Science and Engineering of Materials and Processes (SIMAP). Grenoble Institute of Technology (INGP).
27. Rigaud, V., Daloz, D., Drillet, J., Perlade, A., Maugis, P., Lesoult, G. (2007). Phases Equilibrium Study in Quaternary Iron-rich Fe-Al-Mn-C Alloys. ISIJ International, 47 (6), 898–906. doi: https://doi.org/10.2355/isijinternational.47.898
28. Leslie, W. C., Hornbogen, E. (1996). Physical metallurgy of steels. Physical Metallurgy, 1555–1620. doi: https://doi.org/10.1016/b978-044489875-3/50022-3
29. Huang, B. X., Wang, X. D., Rong, Y. H., Wang, L., Jin, L. (2006). Mechanical behavior and martensitic transformation of an Fe–Mn–Si–Al–Nb alloy. Materials Science and Engineering: A, 438-440, 306–311. doi: https://doi.org/10.1016/j.msea.2006.02.150